AUSTRIAN INSTITUTE OF TECHNOLOGY
TOMORROW TODAY

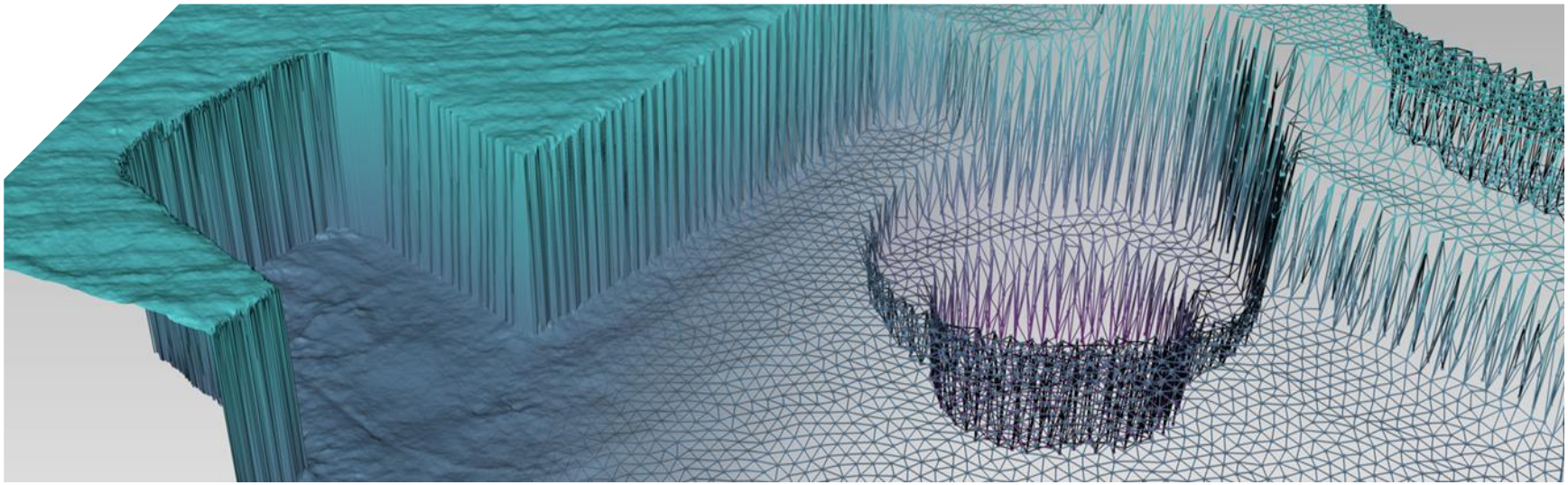

Fusion of Light Field and Photometric Stereo

High precision 3D reconstruction

D. Antensteiner

HIGHLY PRECISE 3D RECONSTRUCTION

For objects with different surface properties (matt, glossy, textureless, …)

The scene
(black zip tie, coin, file)

3D reconstruction using conventional stereo

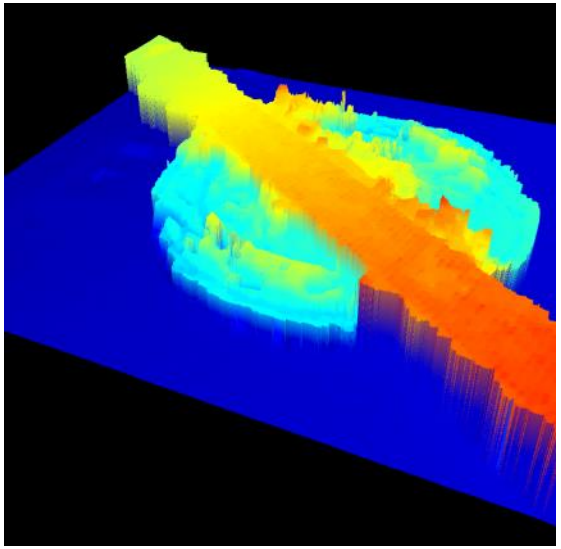

3D reconstruction using light field and photometric stereo

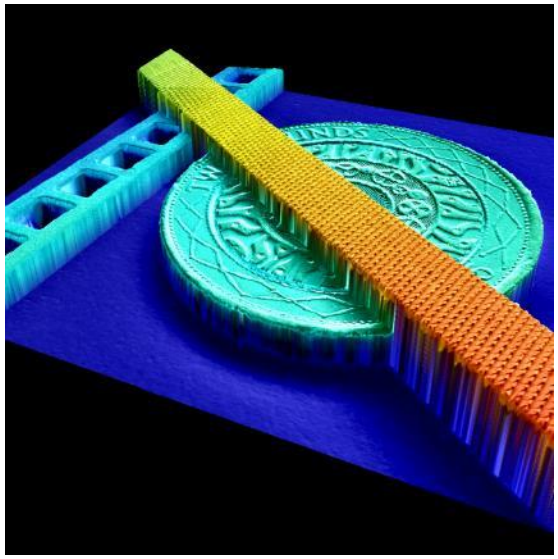

SYNTHESIS OF LIGHT FIELDS & PHOTOMETRIC STEREO

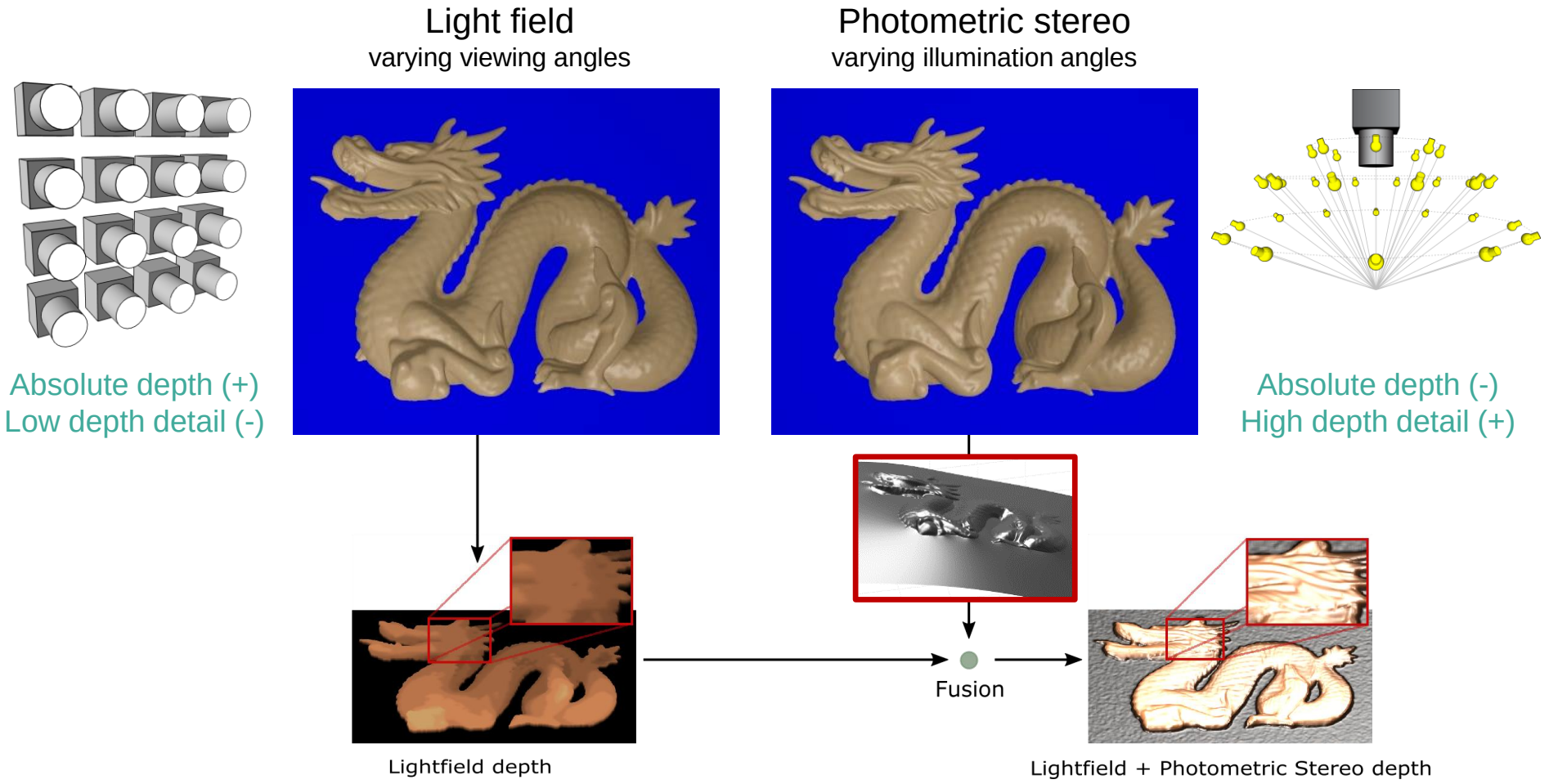

CHALLENGE: INLINE APPLICABILITY

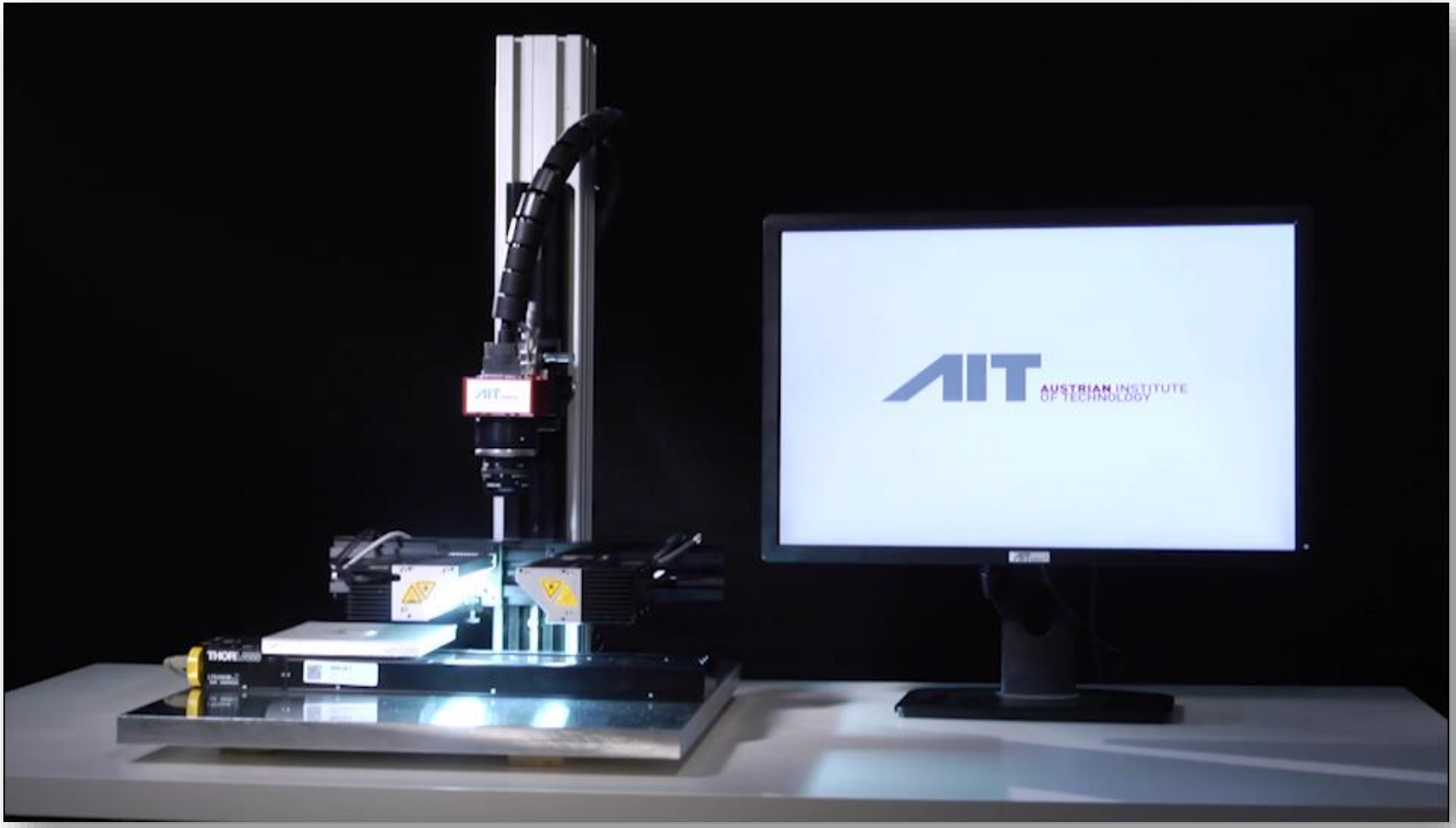

AIT INLINE COMPUTATIONAL IMAGING

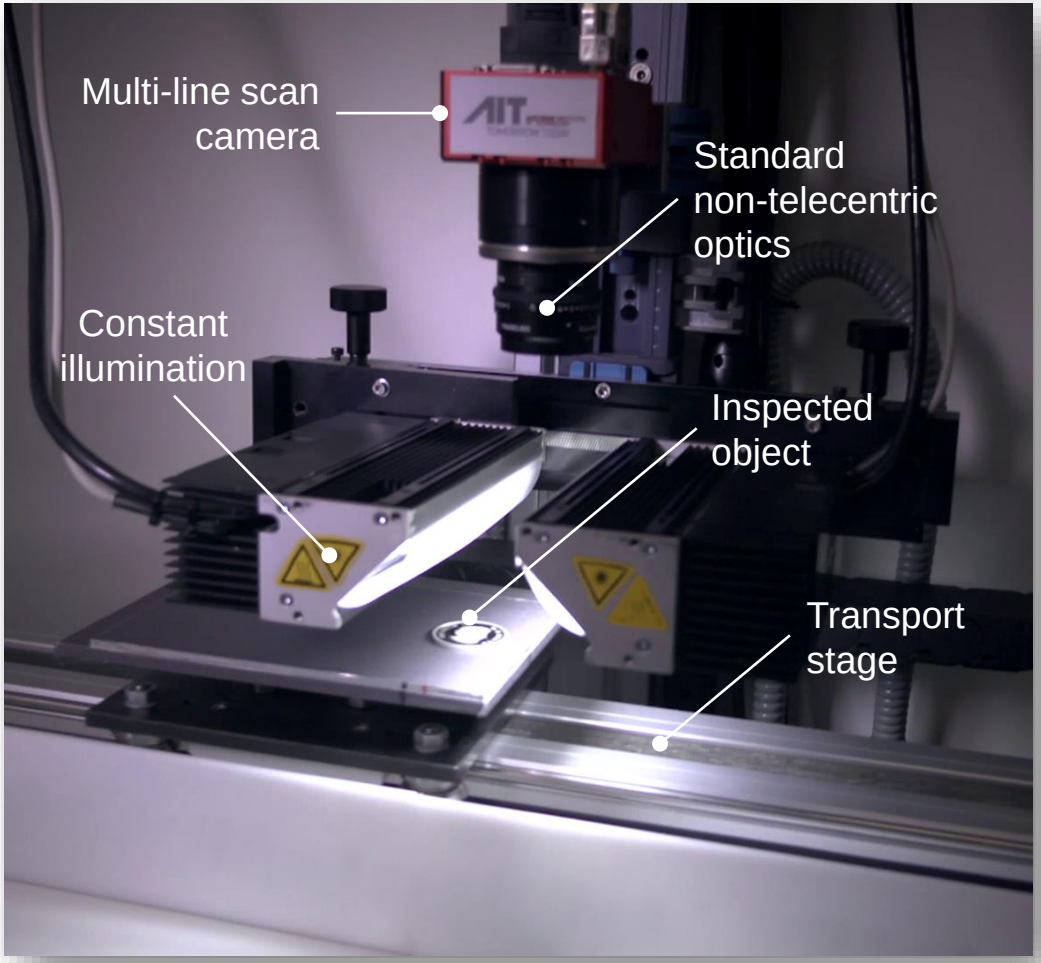

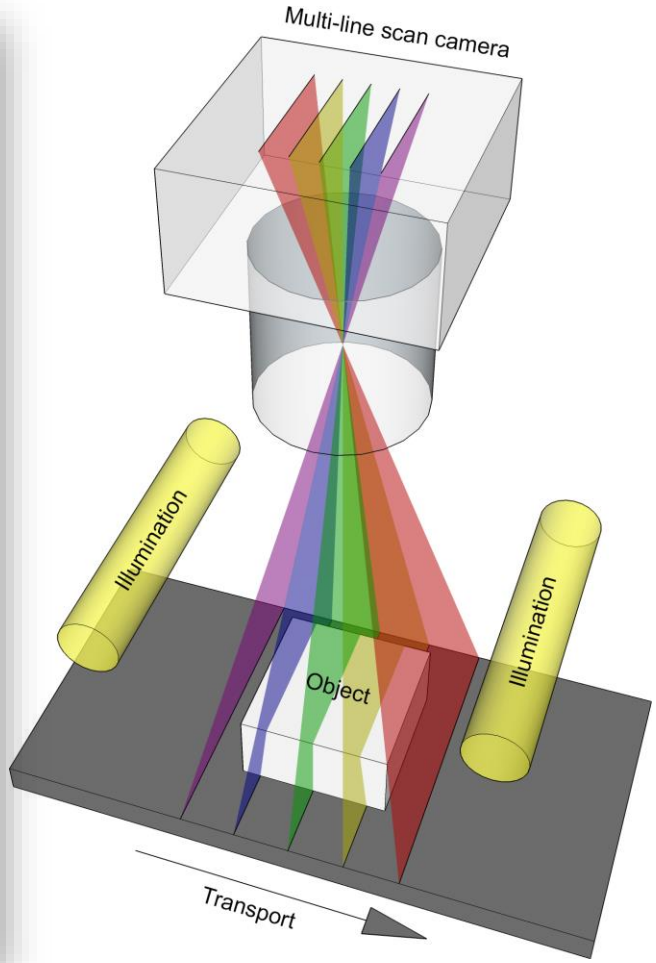

MULTIPLE VIEWING & ILLUMINATION ANGLES

DEPTH FROM LIGHT FIELD USING AIT ICI

- **Multiple views obtained by AIT ICI form a 3D light field of the scene**
- As usual in light field imaging, individual scene points map to lines in the EPI domain
- In AIT ICI, slopes of these lines have linear relationship with depth
  (due to semi-telecentry in the transport direction)
- 3D geometry of the scene can be inferred via multi-view correspondence analysis
  (depth resolution limited due to small baseline)

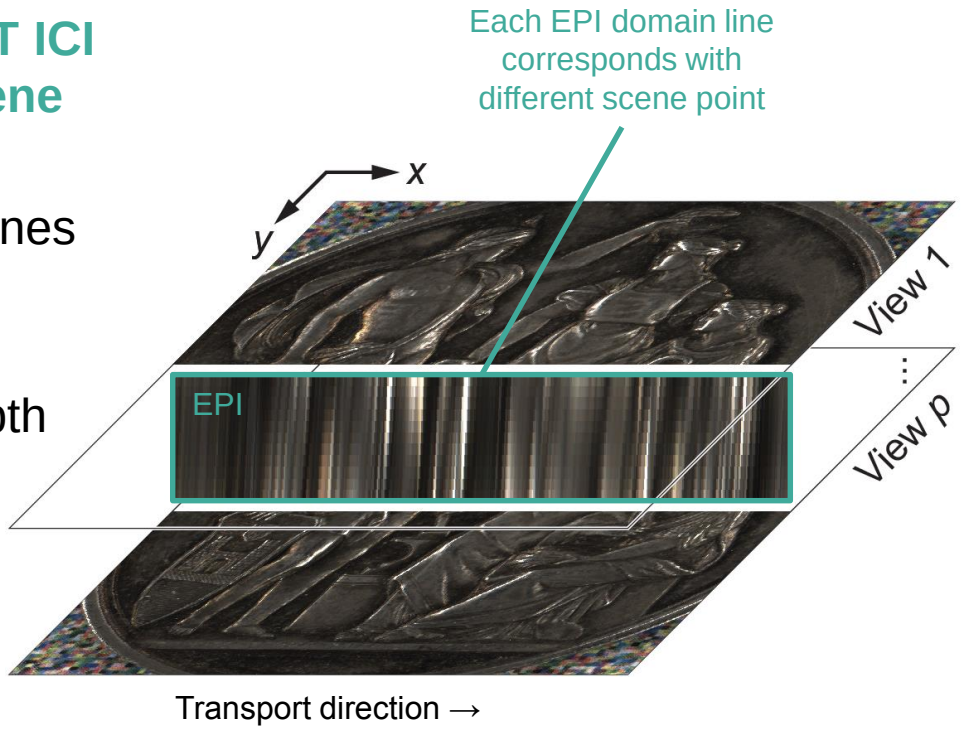

Absolute depth(+)
Low depth detail (-)

PHOTOMETRIC STEREO USING AIT ICI

- **Each light field view contains a different illumination**
- Photometric information associated with a single scene point occur along corresponding EPI line
- To extract this information, an approximate depth model is necessary
  (previously obtained from light field)

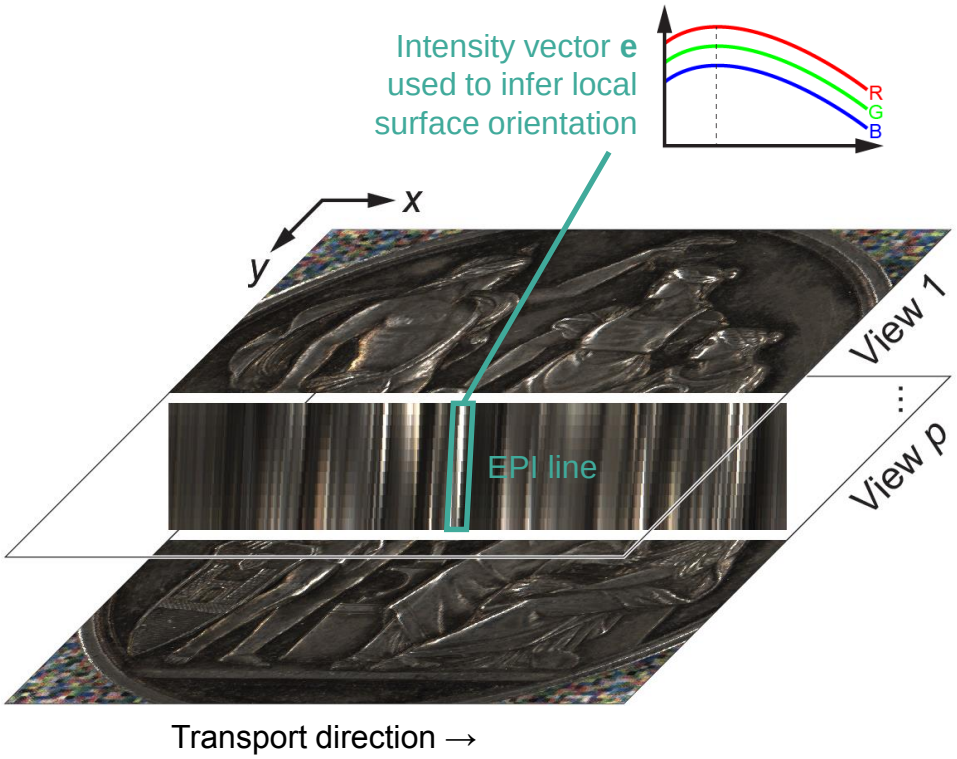

Absolute depth (-)
High depth detail (+)

FUSION

- Optimization problem
- Objective split into two components

$$\min_Z \; ELF(Z)$$

Light field term E_{LF}

Photometric stereo term E_{PS}

$$\min_Z E_{LF}(Z) + E_{PS}(Z)$$

Light field only

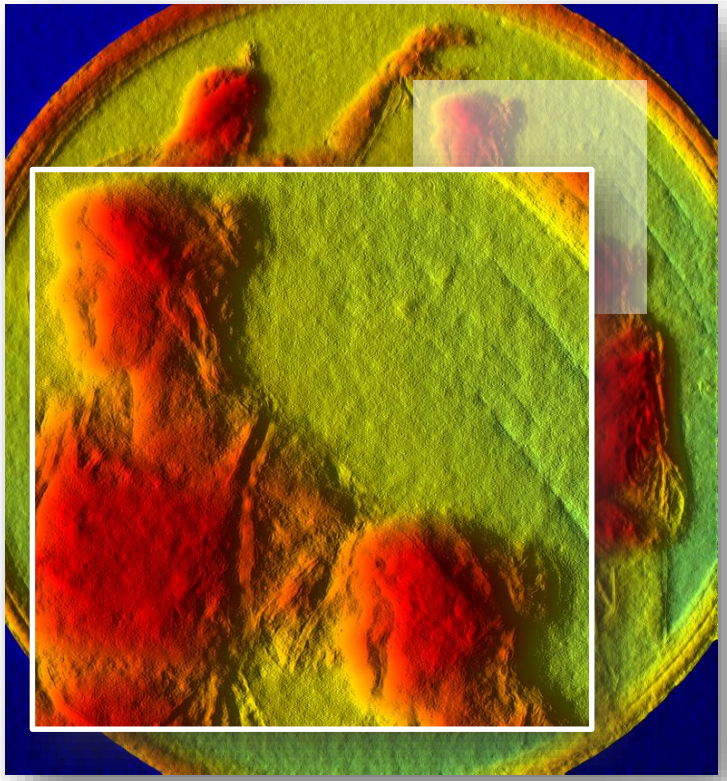

Fusion

NORMAL DISTANCES FOR PHOTOMETRIC STEREO

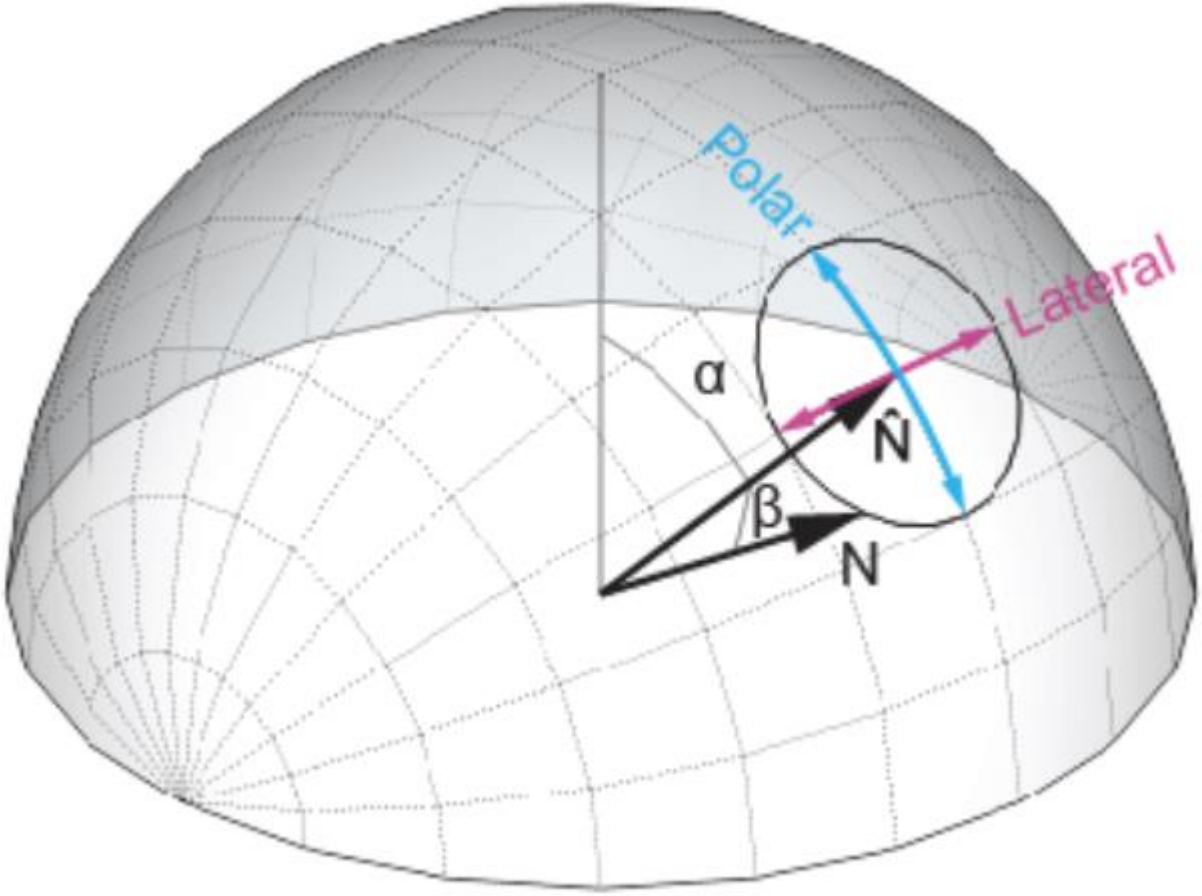

Ideal PS error term (hard to optimize)

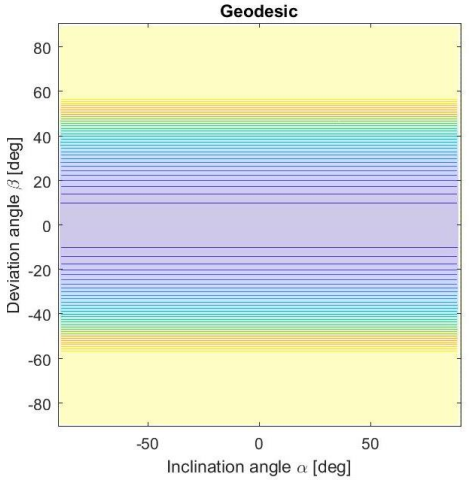

NORMAL DISTANCES – STATE-OF-THE-ART

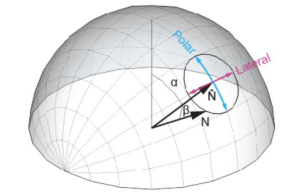

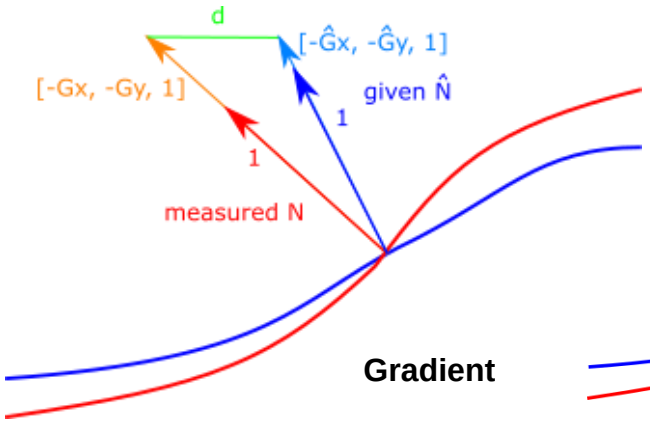

Gradient

$$\min_Z \frac{1}{2}||Z-\hat{Z}||^2+\frac{\lambda}{2}||\nabla Z-\hat{G}||^2$$

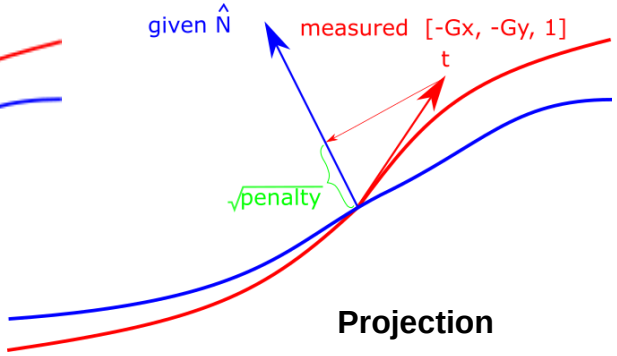

Projection

$$\min_Z \frac{1}{2}||Z-\hat{Z}||^2+\frac{\lambda}{2}\left|\left|\hat{N}_z\odot\nabla_x Z+\hat{N}_x\right|\right|^2+\frac{\lambda}{2}\left|\left|\hat{N}_z\odot\nabla_y Z+\hat{N}_y\right|\right|^2$$

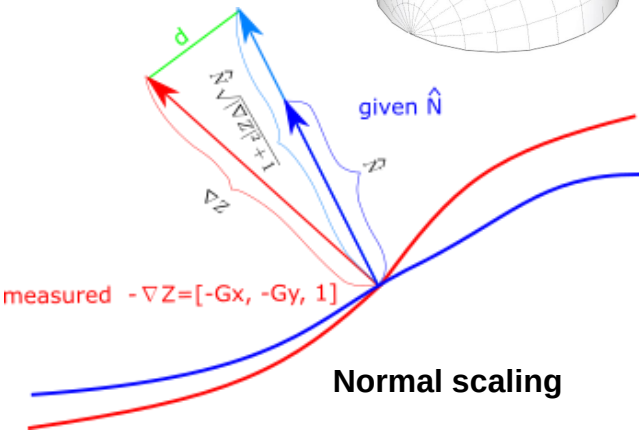

Normal scaling

$$\min_Z \frac{1}{2}||Z-\hat{Z}||^2+\frac{\lambda}{2}\left|\left|(-\nabla Z,1)-\hat{N}\odot|(-\nabla Z,1)|_2\right|\right|_2^2$$

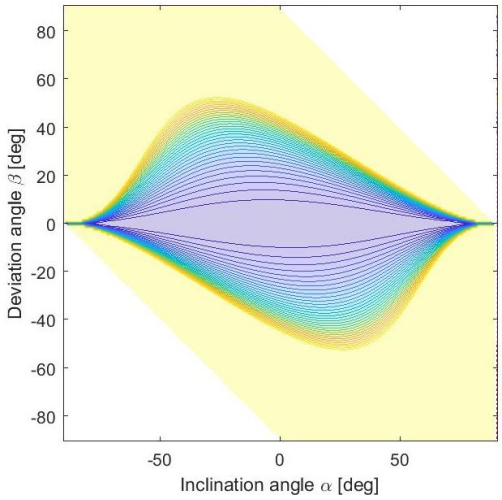

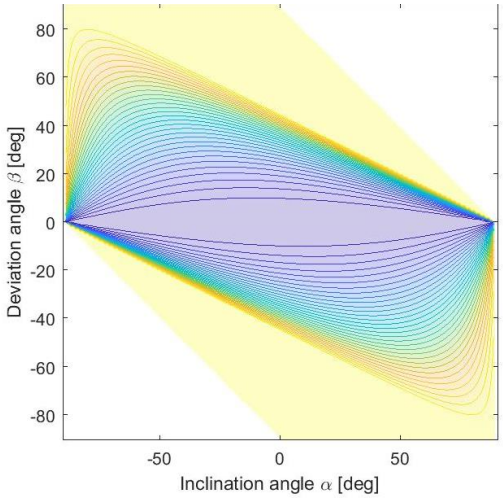

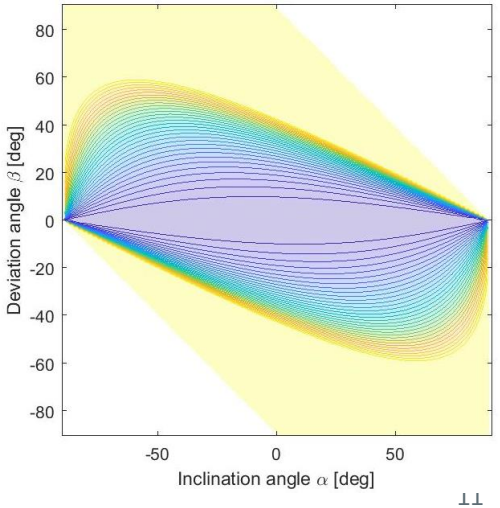

LF + PS FUSION – STATE-OF-THE-ART

Buddha dataset | **Initial Z_{LF}** | **Gradient** | **Projection** | **Normal scaling**

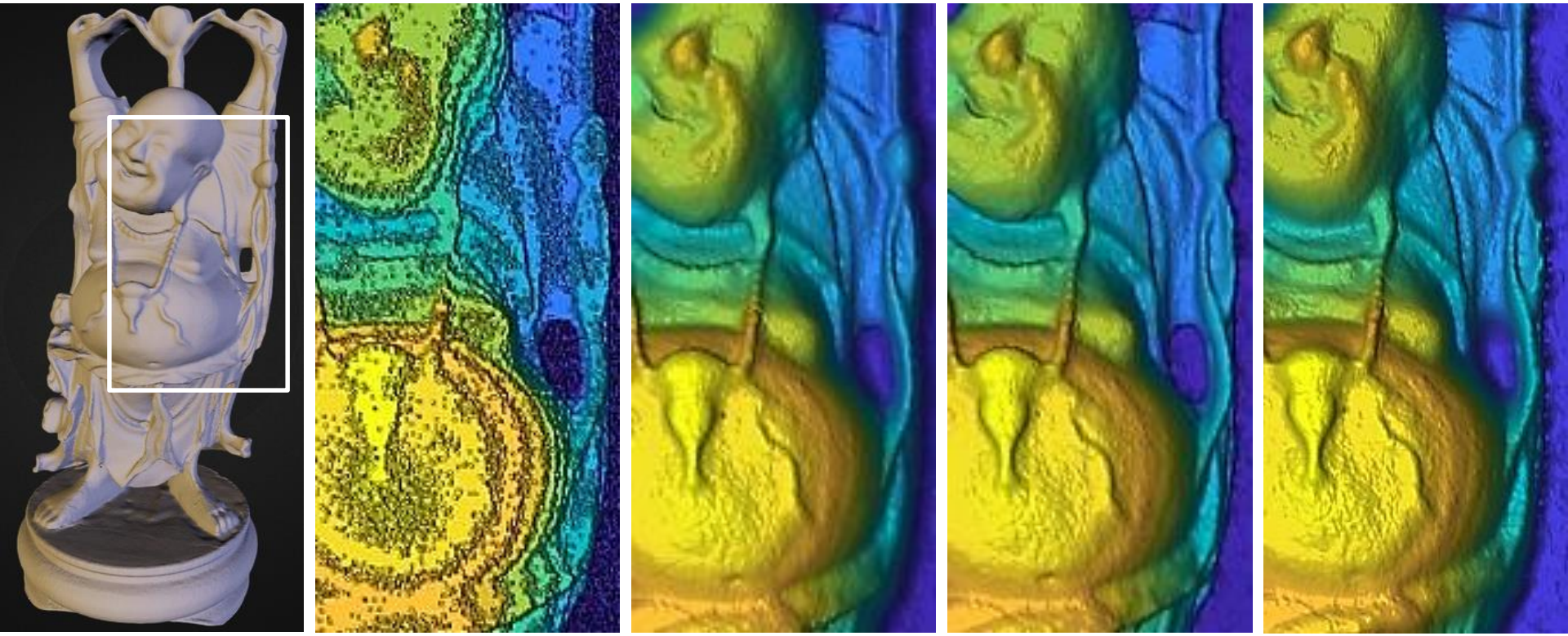

NORMAL DISTANCES – AIT APPROACHES

AIT simple approach

$$\min_{Z} \frac{1}{2}||Z-\hat{Z}||^2 + \frac{\lambda}{2}\left|\left|(\hat{N}_z)^r \odot \nabla_x Z - (\hat{N}_z)^r \odot \hat{G}_x\right|\right|^2 + \frac{\lambda}{2}\left|\left|(\hat{N}_z)^r \odot \nabla_y Z - (\hat{N}_z)^r \odot \hat{G}_y\right|\right|^2$$

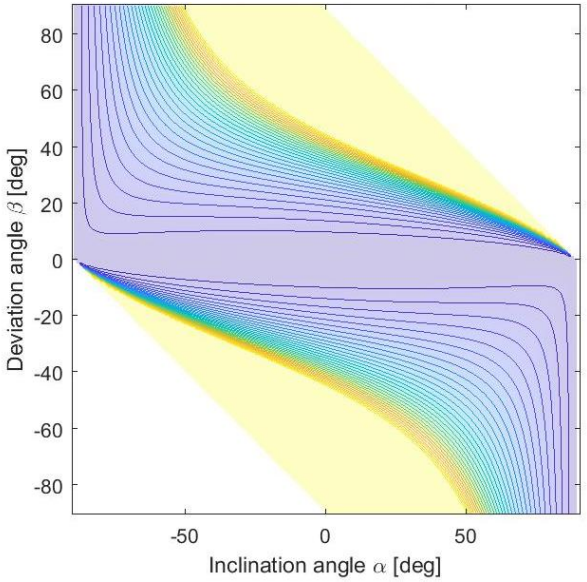

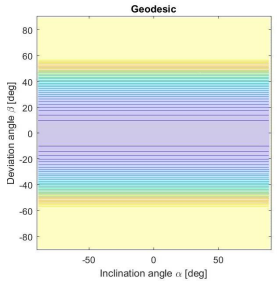

Compare with
the ideal PS error term

AIT TGV regularizer approach

$$\min_{Z,G} \alpha_1||\nabla Z - G||_{2,1} + \alpha_0||\nabla G||_{2,1} + \frac{\alpha}{2}||Z-\hat{Z}||^2 + \frac{\beta}{2}||G-\hat{G}||^2,$$

- Advanced regularization approach using more complex prior
- Accurate yet fast method
- Preserve depth discontinuities
- Minimize staircasing artefacts of other state-of-the-art regularizers

LF + PS FUSION – AIT APPROACHES

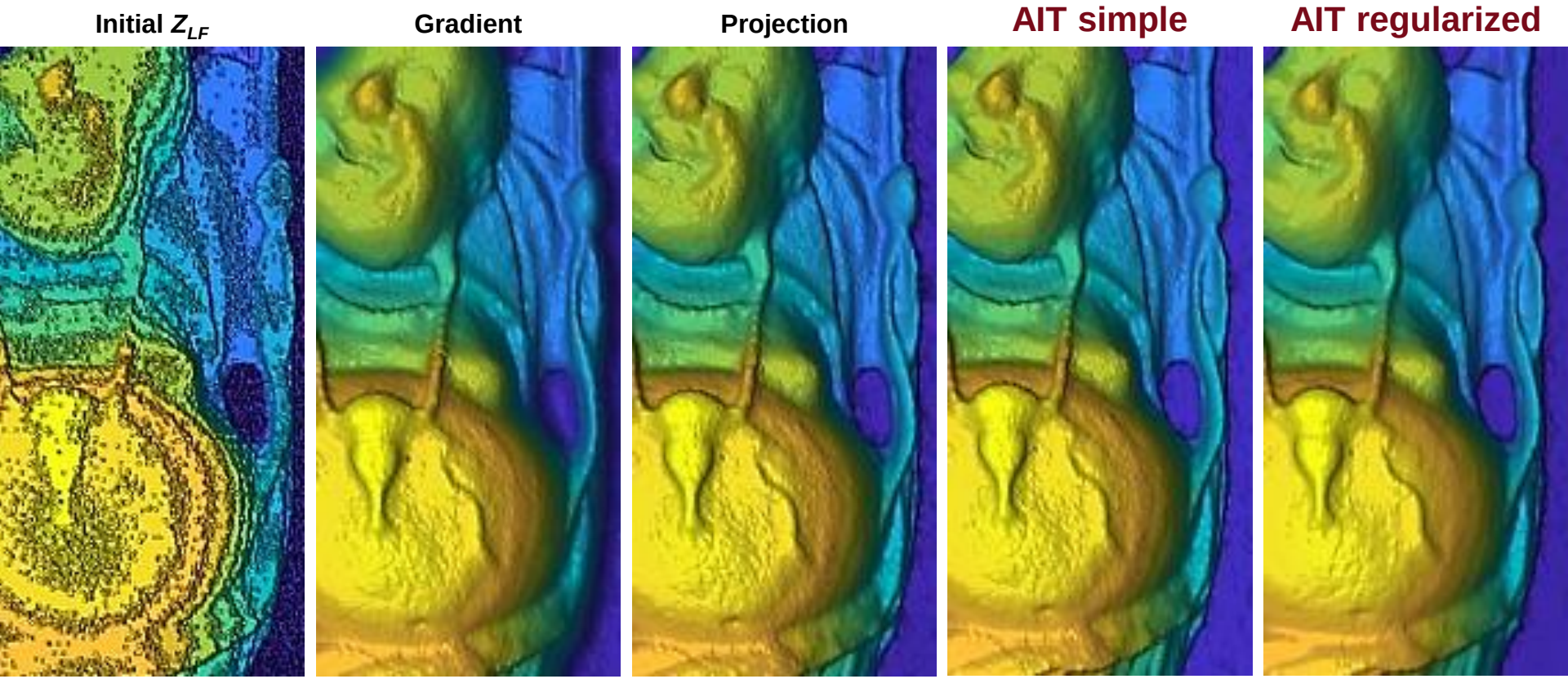

LF + PS FUSION – AIT APPROACHES

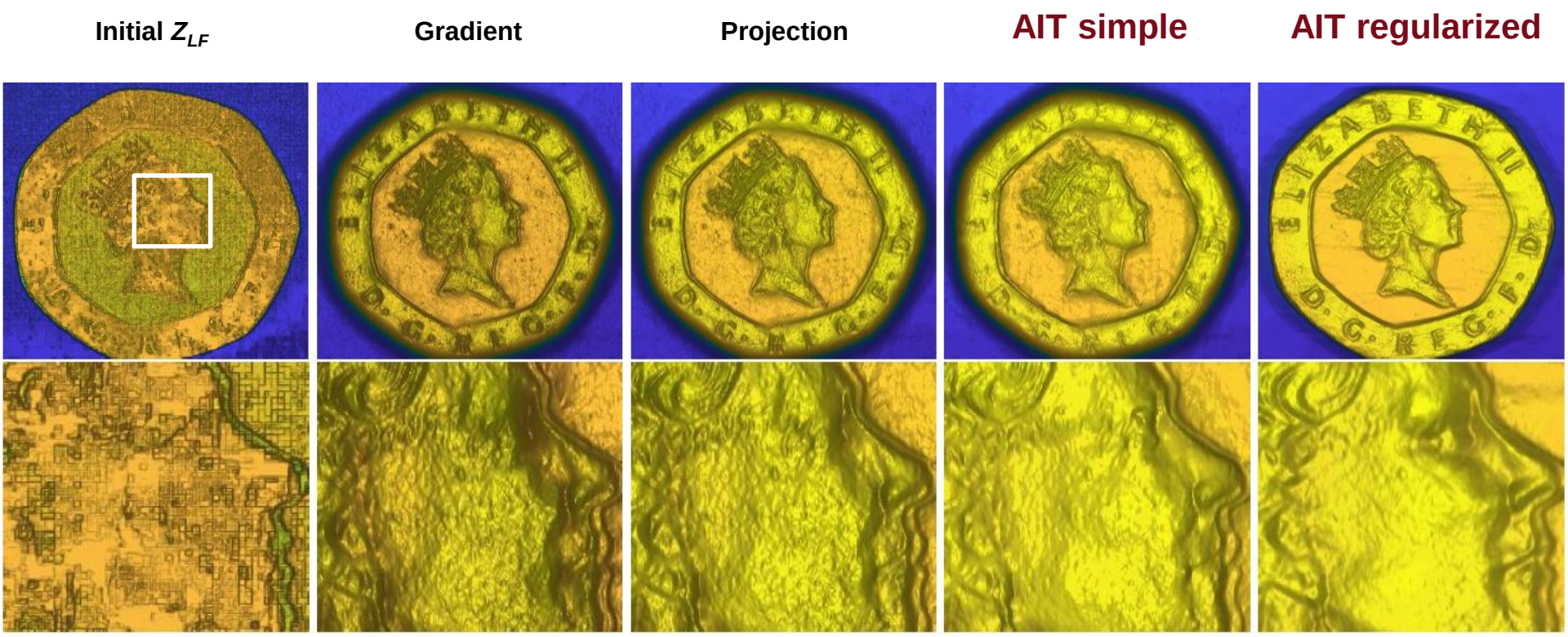

EVALUATION

MSE to the ground truth (Stanford object dataset)

	Dataset \ Method	$\hat{Z}$	Surface orientation only	Gradient based	Projection	Normal Scaling	Ours	Ours with TGV
Depth $[MSE_Z]$	Armadillo	4.23	34.05	2.04	0.13	2.01	**0.10**	0.19
	Buddha	4.85	117.29	2.12	0.15	1.60	**0.12**	0.22
	Dragon	4.60	48.71	1.94	0.13	1.75	**0.10**	0.18
	Avg.	4.53	66.68	1.53	0.14	1.79	**0.11**	0.20
Normals $[GEO_N]$	Armadillo	0.8226	0.2776	0.3205	0.2941	0.3474	0.2849	**0.0664**
	Buddha	0.8767	0.1922	0.2339	0.2102	0.2579	0.2013	**0.0668**
	Dragon	0.8611	0.2397	0.2805	0.2553	0.3094	0.2464	**0.0666**
	Avg.	0.8535	0.2365	0.2783	0.2532	0.3049	0.2442	**0.0666**

Depth map

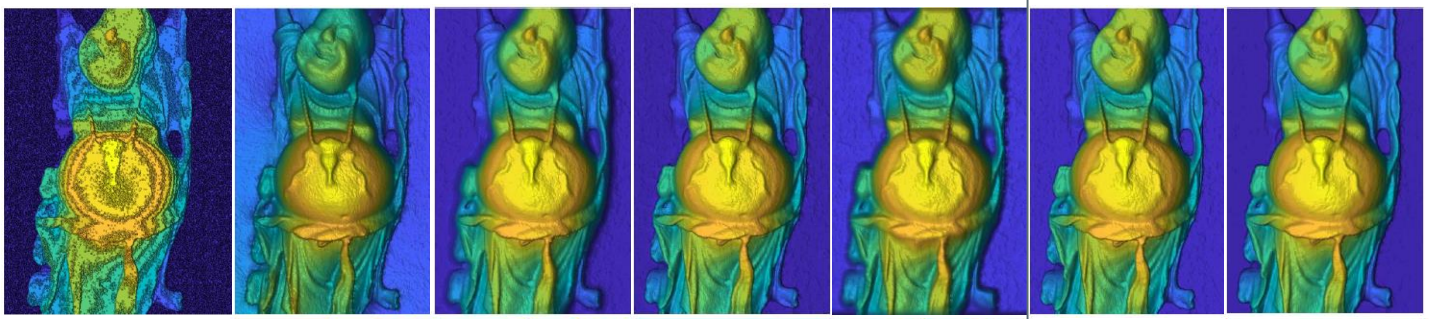

Error map

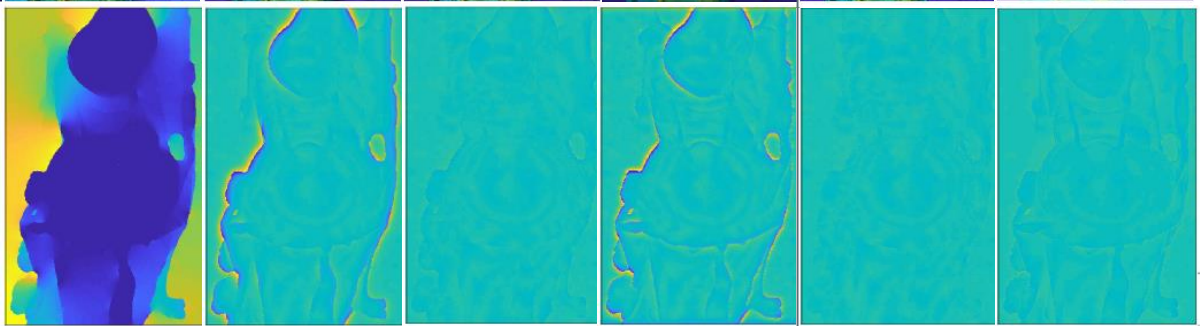

CHIP – INLINE 3D + 2D INSPECTION

Sample part CHIP
(photo)

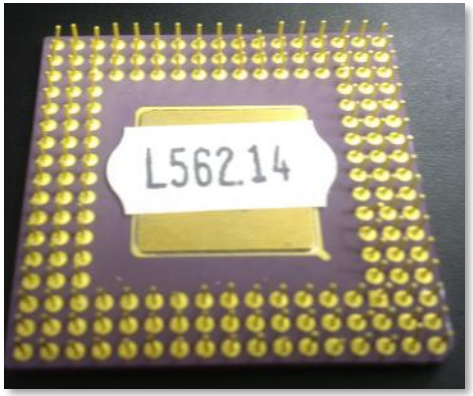

ICI 3D Modell
(pseudo color map)

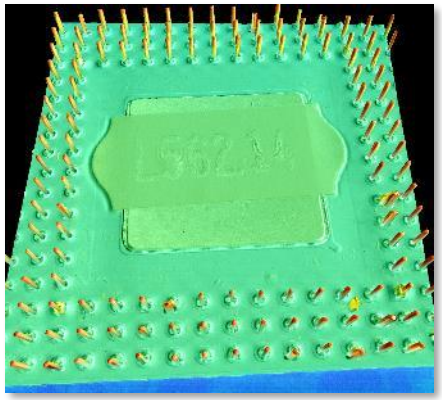

ICI 3D Model + Texture

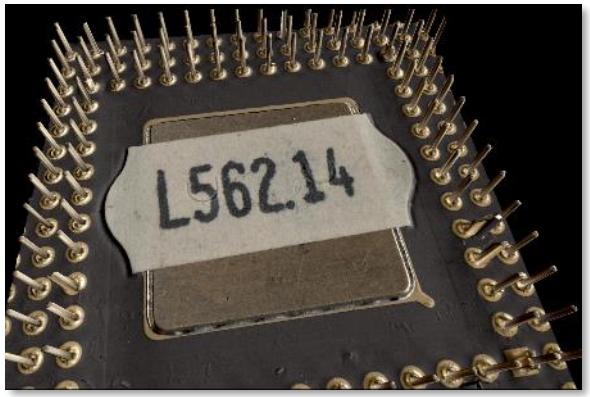

Light field image stack

Detail

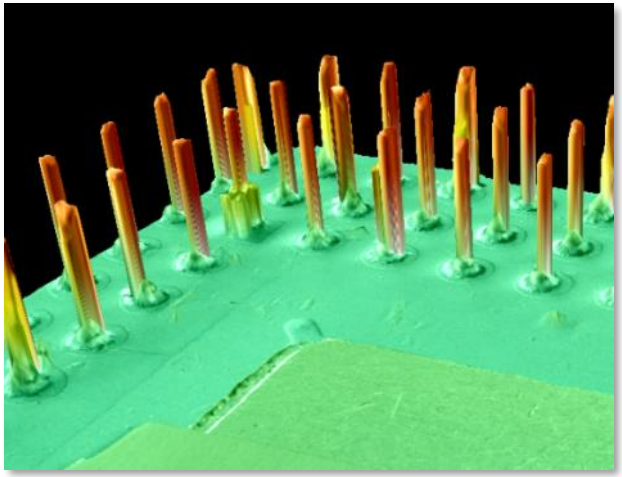

Detail

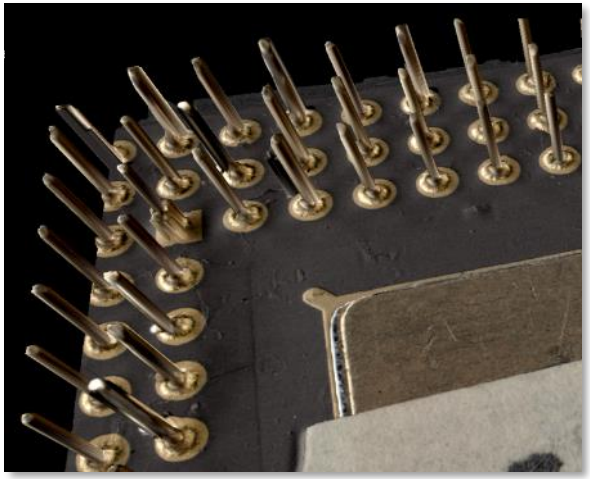

FIELDS OF APPLICATION FOR ICI

Specifically developed for high-performance inline inspection

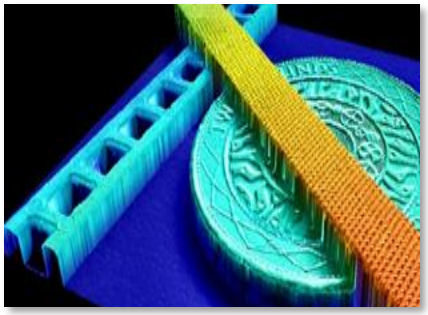

INDUSTRIAL INSPECTION

- 2D and 3D features
- for challenging objects
  - bright / dark
  - matt / glossy
  - texture-less

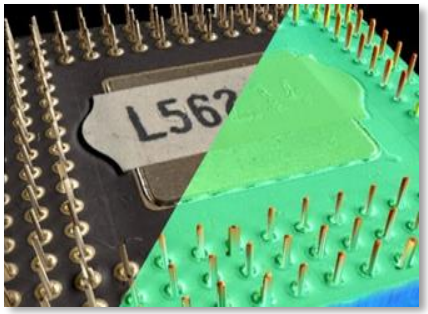

ELECTRONIC PARTS

- PCB and PCB assembly
- solder joints
- pin position and height
- etc.

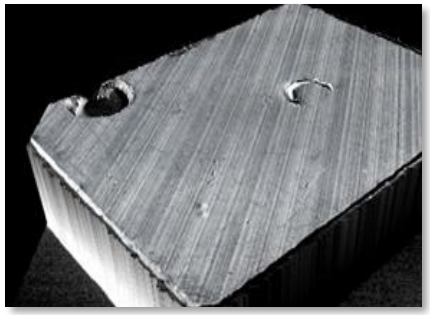

METAL PARTS

- 3D geometry
- surface quality
- detection of pores, cracks, scratches, …
- µm defects

PRINT INSPECTION

- printed matter
- embossing (e.g. braille)
- security features (e.g. holograms)
- tactile elements

Industrial Application

AIT Inline Computational Imaging

- Single multi-line scan camera with constant illumination (low system complexity, low cost)
- Suitable for high-speed inline applications (works with AIT xposure at 100 kHz)
- Suitable for high-resolution (currently 2-50 µm/px)
- High depth accuracy and detail (using light field and photometric stereo, equivalent lateral and depth resolution)
- Extremely flexible (speed vs. accuracy, image enhancement, color, 2D/3D, etc.)
- Future proof (extensible by new technologies beyond light field and photometric stereo)
- World-wide novel technology

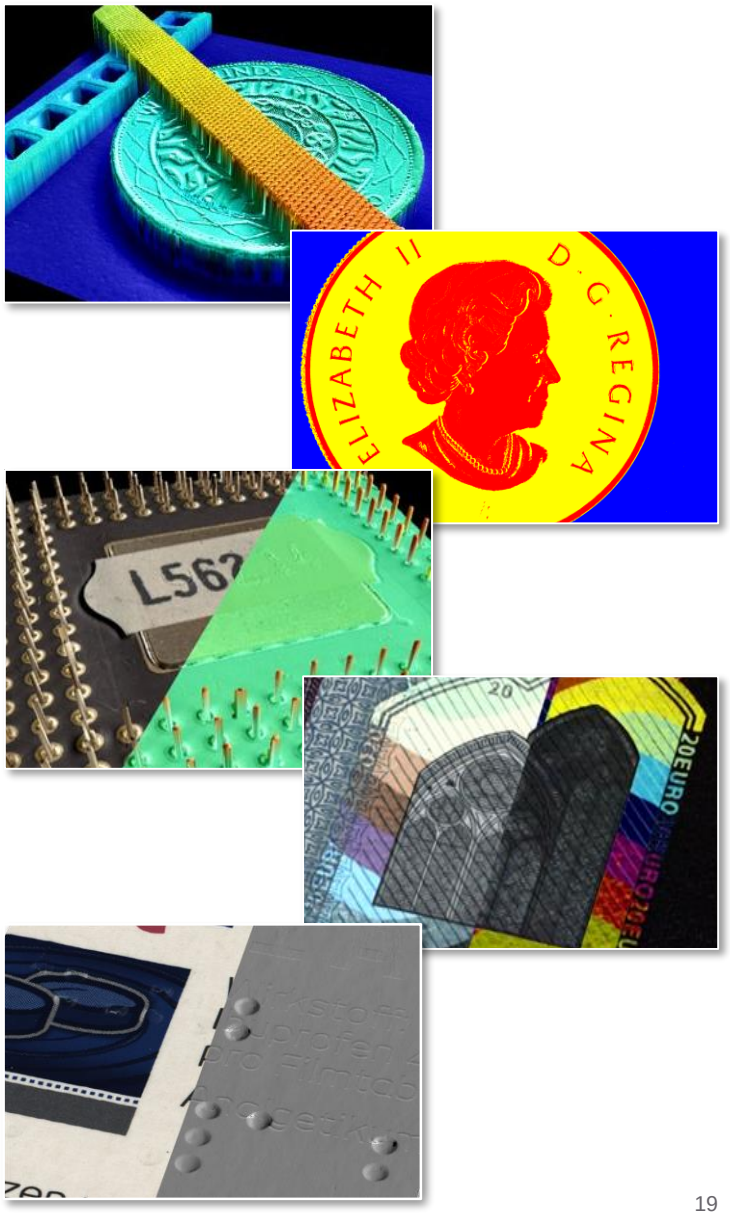

THANK YOU!

Doris Antensteiner
email: doris.antensteiner@ait.ac.at
www.ait.ac.at/hpv